RSC Advances

PAPER

View Article Online
View Journal | View Issue

Cite this: *RSC Adv.*, 2022, **12**, 29892

Highly emissive planarized *B,N*-diarylated benzonaphthoazaborine compounds for narrowband blue fluorescence†

Nhi Ngoc Tuyet Nguyen,‡ Hanif Mubarok,‡ Taehwan Lee, Thi Quyen Tran, Jaehoon Jung * and Min Hyung Lee *

Received 18th August 2022
Accepted 12th October 2022

DOI: 10.1039/d2ra05163j

rsc.li/rsc-advances

Highly fluorescent blue emitters with high color purity are of great significance for optical applications. Herein, a series of planarized *B,N*-diarylated benzonaphthoazaborine compounds, namely, BzNp (**1**), BuBzNp (**2**), Bu_2BzNp (**3**), $Bu_2BzMeNp$ (**4**), and $Bu_2BzBuNp$ (**5**), where electron-donating ^{t}Bu and Me groups are differently introduced into the *B*-Ph, *N*-Ph, or benzoazaborine rings, are prepared and characterized. All compounds exhibit low-energy absorptions (λ_{abs} = 462–467 nm) and emissions (λ_{PL} = 472–478 nm) remarkably red-shifted compared with those found for the pristine dibenzoazaborine compound (404 and 415 nm, respectively). Although the expansion of π-conjugation in the azaborine ring by replacing one phenyl ring with a naphthyl ring is mainly responsible for the redshifts, the emission is also fine-tuned by attached alkyl groups, which have a greater impact on the B-centered LUMO level at the azaborine ring than at the *B*-Ph ring. The bandgap control and emission tuning are further supported by electrochemical and theoretical studies. Notably, blue to sky-blue fluorescence of all compounds exhibits unitary photoluminescence quantum yields, narrow full width at half maximum values (~20 nm), and small Stokes shifts (~11 nm), indicating strong emissions with high color purity.

Introduction

Embedding heteroatoms in polycyclic aromatic hydrocarbons (PAHs) is an effective method for tuning their photophysical properties by modifying their π-orbital interactions, thereby improving the performance of optoelectronic devices, such as organic light-emitting diodes (OLEDs).[1–8] The most widely used strategy is the doping of boron (B) and nitrogen (N) atoms into the PAHs because B and N atoms can exert complementary electron-accepting and electron-donating properties, respectively, on the π-conjugated framework, allowing the modulation of the HOMO and LUMO distributions and their energy gap.[9–18] Among B,N-doped PAHs, the derivatives of *B,N*-diphenyl-5,10-dihydro-dibenzo-1,4-azaborine, namely, dibenzoazaborine,[19,20] have recently attracted significant attention because the dibenzoazaborine skeleton may constitute the main component of highly efficient emitting materials such as thermally activated delayed fluorescence (TADF) compounds.[21,22] More interestingly, B,N-doped PAHs containing multiple azaborine rings have exhibited excellent photophysical properties such as narrowband emissions with high photoluminescence quantum yields (PLQYs) due to the multi-resonance effects of B and N atoms that confine the HOMO and LUMO on different ring atoms.[23,24]

In an effort to extend the feasibility of dibenzoazaborines in optoelectronic applications, Yamaguchi *et al.* have recently disclosed fully planarized dibenzoazaborine structures in which the *B*-Ph ring is tethered with the two Ph rings in the dibenzoazaborine moiety through dimethylmethylene bridges (R^1 = R^2 = H in **A** in Chart 1).[25] It was shown that the chemical and thermal stability of dibenzoazaborines can be improved by structural constraints imposed by a triply-bridged cyclic structure.[4] Furthermore, the planarized polycyclic structure featured

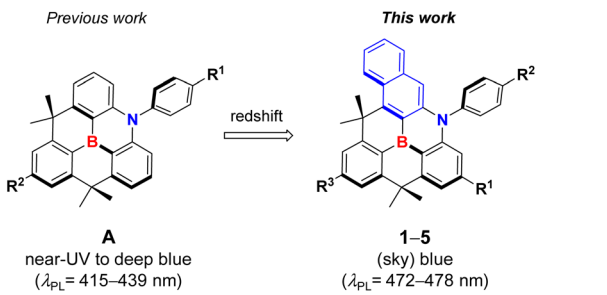

Chart 1 Planarized *B,N*-diarylated benzonaphthoazaborine derivatives (**1–5**).

Department of Chemistry, University of Ulsan, Ulsan 44610, Republic of Korea. E-mail: jjung2015@ulsan.ac.kr; lmh74@ulsan.ac.kr

† Electronic supplementary information (ESI) available: Experimental, photophysical and computational data, and NMR spectra. See DOI: https://doi.org/10.1039/d2ra05163j

‡ These authors contributed equally to this work.

an expanded π-conjugation through the vacant p(B) orbital, which helped strengthen the B–C bonds.[26–28] Interestingly, the planarized dibenzoazaborines exhibited narrowband emissions with full width at half maximum (FWHM) values less than 30 nm.[25] However, the compounds fluoresced at the near UV-region (~415 nm). For practical use in optical applications, emitters should exhibit emissions in the visible region, such as the blue region. For this purpose, we recently reported a series of planarized *B*,*N*-diarylated dibenzoazaborine compounds, where various electronic modifications on the *B*- and/or *N*-aryl groups were performed to control the HOMO–LUMO bandgap while preserving the dibenzoazaborine ring core (*e.g.*, R^1 = H; R^2 = aryl in **A** in Chart 1).[29] Although the emission can be effectively controlled to produce deep blue fluorescence at 421–439 nm, we concluded that the bandgap control by modifying the *B*,*N*-diaryl groups has a limitation, probably due to the simultaneous electronic effects of the *B*- or *N*-aryl substituents on both the HOMO and LUMO levels, partially offsetting the bandgap.

Nonetheless, the preceding results indicate that planarized diarylazaborines are potential candidates for efficient blue emitters with high PLQYs, narrow emission bandwidths, and improved stability compared with typical triarylboryl-based materials. This prompted us to investigate the extension of the emission up to (sky) blue regions. To this end, we decided to modify the central dibenzoazaborine core toward a fused π-conjugated system because the expansion of π-conjugation will have a significant impact on the reduction of the bandgap.[30] In this study, we replaced one phenyl ring in dibenzoazaborine with a naphthyl ring to produce a planarized *B*,*N*-diphenyl benzonaphthoazaborine compound (R^1 = R^2 = R^3 = H; **1** in Chart 1). Furthermore, for the fine-tuning of the emission, we made additional electronic modifications on the *B*-Ph, *N*-Ph, and/or azaborine rings of **1**, which afforded compounds **2–5**. It is shown that all compounds emit blue to sky-blue fluorescence (λ_{PL} = 472–478 nm) in a controlled manner, with unitary PLQYs, very narrow FWHM values (~20 nm), and small Stokes shifts (~11 nm). The details of the synthesis and photophysical properties are described, along with theoretical studies.

Experimental

Synthesis of 1a

The mixture of 2,3-dibromonaphthalene (3.00 g, 10.50 mmol), 2-bromoaniline (1.20 g, 7.00 mmol), tris-(dibenzylideneacetone) dipalladium(0) ($Pd_2(dba)_3$, 0.19 g, 0.21 mmol), bis[(2-diphenylphosphino)phenyl] ether (DPEPhos, 0.23 g, 0.42 mmol), and sodium *tert*-butoxide (NaO^tBu, 1.00 g, 10.5 mmol) in dry toluene (30 mL) was heated at 80 °C for 12 h. After cooling down, the mixture was diluted with CH_2Cl_2 (30 mL), filtered through Celite pad, and concentrated under reduced pressure. The crude product was subjected to silica gel column chromatography using CH_2Cl_2/hexane (1 : 10, v/v) as an eluent to give **1a** as a white solid (yield: 1.40 g, 53%). ^{1}H NMR ($CDCl_3$): δ 8.13 (s, 1H), 7.69 (d, J = 8.4 Hz, 1H), 7.64–7.60 (m, 3H), 7.45 (ddd, J = 13.8, 8.2, 6.8 Hz, 2H), 7.36 (dd, J = 8.1, 1.2 Hz, 1H), 7.30 (dd, J = 7.3, 1.4 Hz, 1H), 6.92–6.86 (m, 1H), 6.62 (br, 1H). ^{13}C NMR ($CDCl_3$): δ 140.1, 137.5, 133.4, 133.4, 132.2, 129.9, 128.3, 127.0, 126.8, 126.6, 124.7, 122.9, 118.6, 115.6, 114.7, 112.7.

Synthesis of 1b

The mixture of **1a** (1.40 g, 3.71 mmol), iodobenzene (3.80 g, 18.60 mmol), copper iodide (0.35 g, 1.86 mmol), and potassium carbonate (1.50 g, 11.13 mmol) was refluxed at 200 °C for 24 h. After cooling to room temperature, CH_2Cl_2 (30 mL) and water (50 mL) were added to the mixture. The organic layer was separated, and the aqueous layer was extracted with CH_2Cl_2 three times (30 mL × 3). The combined organic layer was washed with brine, dried over $MgSO_4$, and concentrated under reduced pressure. The crude product was purified by silica gel column chromatography using CH_2Cl_2/hexane (1 : 10, v/v) as an eluent to give **1b** as a white solid (yield: 1.45 g, 86%). ^{1}H NMR ($CDCl_3$): δ 8.16 (s, 1H), 7.77–7.71 (m, 1H), 7.64 (d, J = 7.0 Hz, 2H), 7.52 (s, 1H), 7.45 (dd, J = 6.0, 3.2 Hz, 2H), 7.23 (dt, J = 19.4, 7.3 Hz, 4H), 7.07 (t, J = 7.5 Hz, 1H), 7.00 (t, J = 7.2 Hz, 1H), 6.78 (d, J = 7.9 Hz, 2H). ^{13}C NMR ($CDCl_3$): δ 147.8, 146.2, 143.2, 134.8, 133.6, 133.2, 132.2, 129.5, 129.1, 128.5, 127.4, 127.1, 126.8, 126.7, 126.5, 126.4, 122.2, 122.0, 121.4, 121.3.

Synthesis of 1c

To a solution of **1b** (1.50 g, 3.31 mmol) in dry THF (30 mL) was added dropwise *n*-BuLi (2.5 M in hexane, 2.65 mL, 6.62 mmol) at −78 °C. The mixture was stirred at −78 °C for 1 h and then Me_2SiCl_2 (0.43 g, 3.31 mmol) was slowly added. After stirring at room temperature overnight, the resulting white turbid mixture was quenched by saturated aqueous NH_4Cl solution (50 mL) and extracted with diethyl ether (30 mL × 3). The combined organic layer was dried over $MgSO_4$, filtered, and concentrated under reduced pressure. The crude product was purified by silica gel column chromatography using CH_2Cl_2/hexane (1 : 10, v/v) as an eluent to give **1c** as a white powder (yield: 0.97 g, 83%). ^{1}H NMR ($CDCl_3$): δ 8.10 (s, 1H), 7.78 (d, J = 7.8 Hz, 1H), 7.70 (dd, J = 10.3, 4.7 Hz, 2H), 7.63–7.54 (m, 2H), 7.43 (d, J = 8.0 Hz, 1H), 7.39–7.35 (m, 2H), 7.33–7.24 (m, 2H), 7.16 (ddd, J = 8.8, 7.2, 1.8 Hz, 1H), 6.99 (dt, J = 7.1, 3.6 Hz, 1H), 6.62 (s, 1H), 6.38 (d, J = 8.6 Hz, 1H), 0.62 (s, 6H). ^{13}C NMR ($CDCl_3$): δ 149.8, 146.9, 144.0, 135.3, 134.8, 134.4, 131.3, 131.2, 130.2, 128.1, 128.0, 127.3, 127.2, 126.7, 123.5, 122.8, 119.8, 119.0, 117.2, 112.1, 0.4.

Synthesis of 1d

Boron tribromide (BBr_3, 0.53 g, 2.10 mmol) was added carefully to the flask containing **1c** (0.25 g, 0.70 mmol) at room temperature. After stirring at 60 °C for 3 h, the volatiles were removed under reduced pressure at the same temperature for 2 h. The crude mixture was dissolved in anhydrous toluene (10 mL), into which a toluene solution of (2,6-di(prop-1-en-2-yl)phenyl) lithium was added at 0 °C. The latter solution was prepared by the addition of *n*-BuLi (2.5 M in hexane, 0.4 mL, 1 mmol) into a toluene solution of 2-bromo-1,3-di(prop-1-en-2-yl)benzene (0.20 g, 0.84 mmol) at 0 °C. After stirring at room temperature for 12 h, the mixture was quenched with saturated NH_4Cl solution and extracted with diethyl ether. The organic layer was dried over $MgSO_4$, filtered, and concentrated under reduced

pressure. The crude product was subjected to silica gel column chromatography using CH_2Cl_2/hexane (1 : 6, v/v) to give **1d** as a yellow solid (yield: 0.10 g, 40%). ^{1}H NMR (CD_2Cl_2): δ 8.47 (s, 1H), 7.84 (d, J = 7.7 Hz, 2H), 7.78 (t, J = 7.3 Hz, 2H), 7.72–7.66 (m, 1H), 7.59 (d, J = 8.2 Hz, 1H), 7.45 (m, 7H), 7.31–7.25 (m, 1H), 7.08–7.00 (m, 2H), 6.70 (d, J = 8.7 Hz, 1H), 4.65 (s, 2H), 4.53 (s, 2H), 1.91 (s, 6H). ^{13}C NMR (CD_2Cl_2): δ 148.2, 148.0, 147.8, 144.5, 142.5, 138.9, 137.6, 136.2, 133.2, 131.5, 129.2, 129.1, 127.9, 127.8, 127.4, 127.3, 125.9, 123.6, 119.4, 117.3, 116.7, 112.3, 112.3, 24.7. ^{11}B NMR (CD_2Cl_2): δ 55.3.

Synthesis of 1 (BzNp)

The mixture of **1d** (0.10 g, 0.22 mmol) and scandium(III) triflate ($Sc(OTf)_3$, 0.22 g, 0.44 mmol) in anhydrous 1,2-dichloroethane (50 mL) was refluxed for 12 h. After cooling down, a saturated aqueous solution of $NaHCO_3$ was added. The organic layer was separated, and the aqueous layer was extracted with CH_2Cl_2. The combined organic layer was dried over $MgSO_4$, filtered, and concentrated under reduced pressure. The crude product was purified through silica gel chromatography using CH_2Cl_2/hexane (1 : 6, v/v) to give **1** as a yellow solid (yield: 0.04 g, 36%). ^{1}H NMR (CD_2Cl_2): δ 8.75 (m, 1H), 7.77 (m, 4H), 7.72–7.65 (m, 3H), 7.54 (t, J = 8.1 Hz, 1H), 7.47–7.39 (m, 5H), 6.97 (s, 1H), 6.48 (d, J = 8.4 Hz, 1H), 2.23 (s, 6H), 1.83 (s, 6H). ^{13}C NMR (CD_2Cl_2): δ 160.3, 156.9, 154.8, 154.1, 147.5, 144.0, 142.5, 138.5, 133.8, 132.6, 131.5, 131.0, 130.1, 129.0, 128.5, 126.4, 124.8, 123.9, 122.5, 117.9, 112.6, 111.9, 44.8, 43.0, 35.0, 33.6. ^{11}B NMR (CD_2Cl_2): δ 43.1. HRMS (EI): m/z $[M]^+$ calcd for $C_{34}H_{28}BN$: 461.2315; found: 461.2313. T_{d_5} = 320 °C.

Synthesis of 2–5

These compounds were prepared in a manner analogous to the synthesis of **1**.

Data for 2 (BuBzNp). Yield = 36%. ^{1}H NMR (CD_2Cl_2): δ 8.78–8.71 (m, 1H), 7.82–7.73 (m, 4H), 7.71–7.64 (m, 2H), 7.54 (t, J = 8.1 Hz, 1H), 7.48–7.38 (m, 5H), 6.95 (s, 1H), 6.46 (d, J = 8.1 Hz, 1H), 2.23 (s, 6H), 1.83 (s, 6H), 1.51 (s, 9H). ^{13}C NMR (CD_2Cl_2): δ 160.0, 157.1, 155.7, 154.4, 154.3, 147.5, 144.0, 142.6, 138.5, 133.6, 131.5, 131.1, 130.1, 129.0, 128.5, 126.3, 125.4, 122.4, 121.9, 121.1, 117.9, 112.5, 111.8, 45.1, 43.2, 36.1, 35.1, 33.7, 31.8. ^{11}B NMR (CD_2Cl_2): δ 44.6. HRMS (EI): m/z $[M]^+$ calcd for $C_{38}H_{36}BN$: 517.2941; found: 517.2936. T_{d_5} = 313 °C.

Data for 3 (Bu_2BzNp). Yield = 48%. ^{1}H NMR (CD_2Cl_2): δ 8.74 (m, 1H), 7.79 (dd, J = 5.5, 1.7 Hz, 2H), 7.75 (dd, J = 4.4, 1.7 Hz, 2H), 7.70 (dd, J = 6.4, 3.4 Hz, 1H), 7.54 (t, J = 8.1 Hz, 1H), 7.47–7.38 (m, 3H), 7.38–7.33 (m, 2H), 6.99 (s, 1H), 6.48 (d, J = 8.1 Hz, 1H), 2.23 (s, 6H), 1.83 (s, 6H), 1.51 (s, 9H), 1.50 (s, 9H). ^{13}C NMR (CD_2Cl_2): δ 159.9, 157.1, 155.6, 154.3, 154.3, 152.1, 147.6, 144.1, 139.7, 138.5, 133.6, 130.2, 130.1, 128.5, 128.4, 126.2, 125.3, 122.4, 121.9, 121.1, 117.8, 112.6, 111.8, 45.0, 43.2, 36.1, 35.2, 35.1, 33.7, 31.8, 31.7. ^{11}B NMR (CD_2Cl_2): δ 41.2. HRMS (EI): m/z $[M]^+$ calcd for $C_{42}H_{44}BN$: 573.3567; found: 573.3569. T_{d_5} = 328 °C.

Data for 4 (Bu_2BzMeNp). Yield = 32%. ^{1}H NMR (CD_2Cl_2): δ 8.73 (dd, J = 6.8, 3.5 Hz, 1H), 7.80–7.72 (m, 4H), 7.68 (dd, J = 6.5, 3.4 Hz, 1H), 7.44–7.39 (m, 2H), 7.36–7.31 (m, 2H), 7.24 (s, 1H), 6.93 (s, 1H), 6.33 (s, 1H), 2.39 (s, 3H), 2.22 (s, 6H), 1.82 (s, 6H), 1.51 (d, J = 2.9 Hz, 18H). ^{13}C NMR (CD_2Cl_2): δ 159.9, 157.0, 155.6, 154.2, 152.1, 147.6, 144.3, 144.1, 139.6, 138.4, 133.5, 130.2, 130.0, 128.5, 128.4, 126.2, 125.2, 122.3, 121.8, 121.1, 117.7, 112.5, 111.7, 45.0, 43.1, 36.0, 35.2, 35.1, 33.6, 31.8, 31.6, 21.1. ^{11}B NMR (CD_2Cl_2): δ 44.7. HRMS (EI): m/z $[M]^+$ calcd for $C_{43}H_{46}BN$: 587.3723; found: 587.3722. T_{d_5} = 331 °C.

Data for 5 (Bu_2BzBuNp). Yield = 35%. ^{1}H NMR (CD_2Cl_2): δ 8.74 (dd, J = 6.5, 3.6 Hz, 1H), 7.76 (dd, J = 8.5, 5.7 Hz, 4H), 7.70 (dd, J = 6.3, 3.5 Hz, 1H), 7.46 (d, J = 1.0 Hz, 1H), 7.44–7.39 (m, 2H), 7.36 (d, J = 8.4 Hz, 2H), 7.02 (s, 1H), 6.48 (d, J = 1.0 Hz, 1H), 2.23 (s, 6H), 1.83 (s, 6H), 1.51 (d, J = 0.8 Hz, 18H), 1.25 (s, 9H). ^{13}C NMR (CD_2Cl_2): δ 159.8, 157.2, 156.3, 155.4, 154.5, 154.1, 152.1, 147.7, 144.3, 139.7, 138.5, 130.3, 130.1, 128.5, 128.2, 126.1, 125.2, 122.3, 121.8, 121.2, 115.6, 111.7, 109.7, 45.1, 43.3, 36.0, 36.0, 35.2, 33.6, 31.8, 31.6, 31.3. ^{11}B NMR (CD_2Cl_2): δ 45.7. HRMS (EI): m/z $[M]^+$ calcd for $C_{46}H_{52}BN$: 629.4193; found: 629.4193. T_{d_5} = 337 °C.

Photophysical measurements

UV/Vis absorption and photoluminescence (PL) spectroscopic studies were performed on a Varian Cary 100 and FS5 spectrophotometer (Edinburgh Instruments), respectively. PLQYs (Φ_{PL}) were measured on an absolute PLQY spectrophotometer (Quantaurus-QY C11347-11, Hamamatsu Photonics). Transient PL decay profiles were recorded on a FS5 spectrophotometer using an EPL-375 picosecond pulsed diode laser as an excitation light source.

Results and discussion

Synthesis and characterization

Following analogous methods for preparing previous *B*,*N*-diarylated dibenzoazaborine compounds (**A**),[25,29] planarized *B*,*N*-diarylated benzonaphthoazaborine compounds (**1–5**) were synthesized, as illustrated in Scheme 1. To fine-tune the HOMO–LUMO bandgap (E_g), which is relevant to emission control, we made electronic modifications at the three positions of the parent *B*,*N*-diphenyl benzonaphthoazaborine compound (BzNp, **1**), that is, 4-positions of the *B*-Ph (R^3) and *N*-Ph (R^2) rings and the para position to the B atom of the benzoazaborine core (R^1). As noted previously, the substituents on the *B*-Ph and *N*-Ph rings will mainly affect the LUMO and HOMO, respectively. It is also anticipated that the R^1 substituent may have more influence on the B-centered LUMO level owing to its para-connectivity with the B atom. Therefore, for compounds **1–5**, the incorporated naphthyl ring will mainly control E_g values, which will be then fine-tuned by the R^1–R^3 substituents. We chose electron-donating alkyl groups such as ^{t}Bu and Me groups as the substituents and prepared compounds **1–5**, namely, BzNp (**1**), BuBzNp (**2**), Bu_2BzNp (**3**), Bu_2BzMeNp (**4**), and Bu_2BzBuNp (**5**), in combination with the different number and position of the substituents. First, 3-bromo-*N*-(2-bromophenyl)naphthalen-2-amine intermediates (**1a**, **4a**, and **5a**) were prepared by the Buchwald–Hartwig amination of 2,3-dibromonaphthalene with 2-bromoanilines.

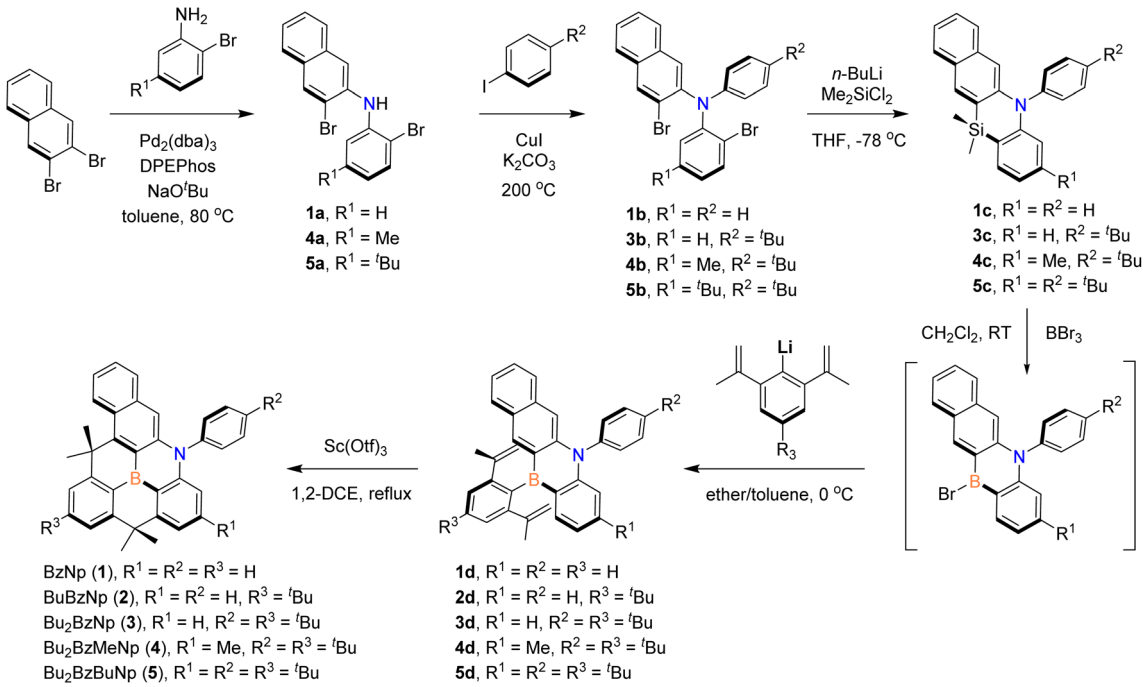

Scheme 1 Synthetic routes for **1**–**5**.

Ullmann coupling of **1a**, **4a**, and **5a** with aryl iodides produced the corresponding 3-bromo-*N*-(2-bromophenyl)-*N*-arylnaphthalen-2-amines (**1b** and **3b**–**5b**), which were then silylated with Me_2SiCl_2 after dilithiation.

Note that the use of the THF solvent led to high yields (>73%) of silanes (**1c** and **3c**–**5c**). However, in the ether solvent, which was used to synthesize previous dibenzoazaborine compounds (**A**),[29] several unknown products, including naphthyl–phenyl coupled species, were formed, consequently resulting in low yields. Next, the silicon–boron exchange reactions of silanes with BBr_3 furnished bromo-azaborine intermediates, which were then subject to *in situ* reactions with 2,6-di(propen-2-yl) phenyllithium[26] or 4-^{t}Bu-2,6-di(propen-2-yl)phenyllithium to yield arylated benzonaphthoazaborines (**1d**–**5d**). The final planarized *B*,*N*-diarylated benzonaphthoazaborines **1**–**5** were obtained *via* twofold intramolecular Friedel–Crafts cyclization reactions in the presence of $Sc(OTf)_3$.[31] All compounds were chemically stable under ambient conditions in solution and solid states. They also exhibited high thermal stability, as judged by high thermal decomposition temperatures (T_{d_5}) above 310 °C (Fig. S1†). Notably, T_{d_5} values increased with an increasing number of alkyl substituents, probably due to the increased steric protection of the planarized azaborine core. The chemical structures of the compounds were characterized by multinuclear NMR spectroscopy and high-resolution mass spectrometry. The broad ^{11}B NMR resonances at δ *ca.* 41–45 ppm, similar to those observed for **A**, confirmed the presence of a trigonal boron atom of the benzonaphthoazaborine skeleton.[25,29]

Photophysical and electrochemical properties

To investigate the photophysical properties of compounds, UV/Vis absorption and photoluminescence (PL) spectra were measured in a toluene solution, and the corresponding spectra are shown in Fig. 1 and S2.† The detailed spectroscopic data are summarized in Table 1. All compounds exhibit similar absorptions in the two regions, that is, the high-energy region at *ca.* 280–340 nm and the low-energy region at *ca.* 400–490 nm. The bands are highly structured, indicating the involvement of the $\pi\pi^*$ state in the transition. The former bands can be primarily attributed to the local $\pi\pi^*$ states of the naphthyl and phenyl rings, whereas the latter is assignable to the $\pi\pi^*$ states, corresponding to the HOMO–LUMO transition, centered on the benzonaphthoazaborine core (see the DFT results below). The lowest energy absorption peak for unsubstituted **1** appeared at 467 nm, which was remarkably red-shifted, compared with the peak (404 nm) for the pristine dibenzoazaborine compound ($R^1 = R^2 = H$ in **A**).[25] This indicates that the incorporation of a naphthyl ring into the azaborine core has a significant impact on the reduction in the bandgap. The introduction of the para alkyl substituents (R^3 and R^1) with respect to the B-atom resulted in gradual blueshifts of the absorption peaks because of the elevation of the LUMO level. Attaching a ^{t}Bu group (R^2) to the *N*-Ph ring resulted in a slight redshift (**2** *vs.* **3**), but the effect was less than that of the blueshift by a ^{t}Bu group on the *B*-Ph ring (**1** *vs.* **2**). Although not strong, these results indicate that the low-energy absorption wavelength, that is, the HOMO–LUMO bandgap, can be fine-tuned by introducing alkyl substituents into the *B*-Ph, *N*-Ph, and/or benzonaphthoazaborine rings.

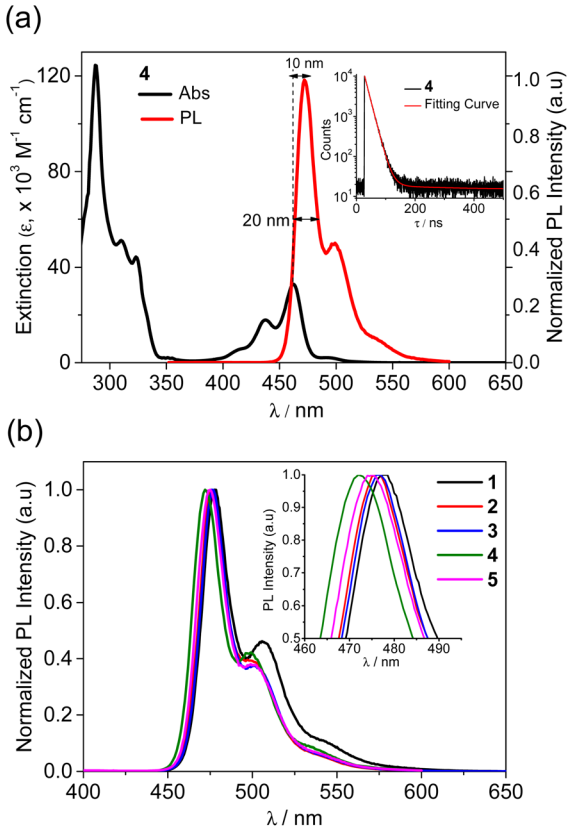

Fig. 1 (a) UV/vis absorption and PL spectra of **4** and (b) PL spectra of **1–5** in toluene (2.0×10^{-5} M) at RT. Insets: (a) transient PL decay of **4** and (b) enlarged PL spectra showing FWHM.

Cyclic voltammetry (CV) was used to examine the electrochemical properties of **1–5** to confirm the bandgap control and HOMO/LUMO energy levels (Fig. 2 and Table 1 and S1†). The oxidation processes revealed that the compounds underwent reversible oxidation centered on benzonaphthoaza moieties (see DFT results below). Compared with the oxidation potential (0.52 V) of unsubstituted **1**, the introduction of alkyl groups gradually reduces the oxidation potential by *ca.* 0.01–0.08 V. The decrease in the potential was the most apparent for compounds with the ^{t}Bu group on the *N*-Ph moiety (**3–5**), which is due to the elevation of the N-centered HOMO level by the electron-donating ^{t}Bu group. The R^1 substituents on the azaborine core also slightly affect the HOMO level (**4** and **5**). Meanwhile,

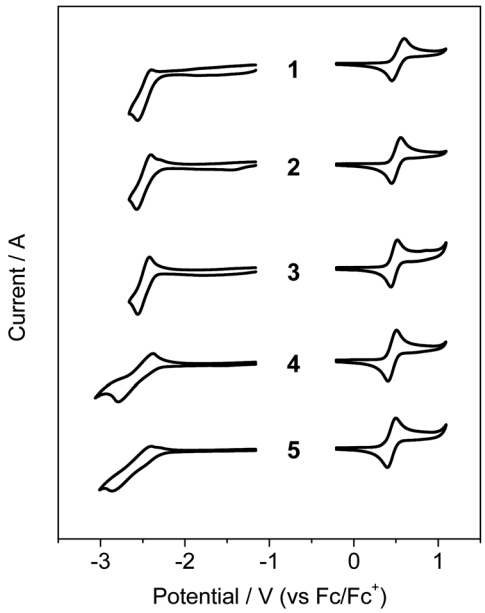

Fig. 2 Cyclic voltammograms of **1–5**. Solvent: CH_2Cl_2 for oxidation and THF for reduction (5.0×10^{-4} M).

the compounds underwent reversible (**1–3**) or quasi-reversible (**4** and **5**) reductions centered on the boron atom. The reduction potential was very slightly shifted cathodically upon the introduction of the ^{t}Bu group on the B-Ph moiety (**2** and **3** *vs.* **1**). However, relatively large cathodic shifts in the reduction potentials by *ca.* 0.09–0.12 V occurred for compounds with the R^1 substituents on the azaborine core (**4** and **5** *vs.* **3**). This implies that the electron-donating effect on the B-centered LUMO level is greater at the azaborine ring than at the *B*-Ph ring. These electrochemical results indicate that the electronic effects of substituents are more obvious in the azaborine ring core than in the *B*-Ph and *N*-Ph moieties, probably due to the localization of frontier molecular orbitals on the conjugated azaborine π-framework. As a result, the electrochemical bandgaps of the compounds were fine-tuned with the greater values for **4** and **5**, as similarly observed in the absorptions. It is noteworthy that the bandgap of **1** is largely decreased by 0.48 eV compared with that (3.48 eV) of dibenzoazaborine compound ($R^1 = R^2 = H$ in **A**)[25] due to the elevated HOMO and lowered LUMO levels (see also the DFT results below).

Table 1 Photophysical Data of **1–5**

Compd	λ_{abs}[a] (nm) ($\varepsilon \times 10^{-3}$/M^{-1} cm^{-1})	λ_{PL}[a] (nm)	Φ_{PL}[a,b] (%)	Stokes shift (nm)	FWHM[a,c] (nm)	τ[a,d] (ns)	HOMO/LUMO[e] (eV)	E_g[f] (eV)
1	285 (57.82), 442 (7.22), 467 (13.17)	478	~100	11	20	17.6	−5.32/−2.32	3.00
2	285 (84.32), 440 (15.09), 466 (27.38)	477	~100	11	20	16.7	−5.31/−2.31	3.00
3	285 (60.19), 441 (9.83), 466 (18.51)	477	~100	11	19	16.3	−5.28/−2.30	2.98
4	287 (124.95), 437 (18.34), 462 (33.51)	472	~100	10	20	15.2	−5.26/−2.21	3.05
5	288 (53.18), 438 (12.41), 464 (22.16)	475	~100	11	20	15.1	−5.24/−2.18	3.06

[a] In oxygen-free toluene at 298 K (2.0×10^{-5} M). [b] Absolute PLQYs ($\lambda_{exc} = 335$ nm). [c] Full width at half maximum. [d] PL lifetimes. [e] Estimated from the electrochemical oxidation (HOMO) and reduction (LUMO). [f] Electrochemical bandgap.

Next, the emission properties of all compounds (**1–5**) were investigated in toluene at room temperature (Fig. 1 and Table 1). Unsubstituted **1** exhibited a sky-blue emission at 478 nm, which is significantly red-shifted compared with that (415 nm) of the dibenzoazaborine compound ($R^1 = R^2 = H$ in **A**).[25] As observed in the absorption, this finding again indicates the impact of the naphthyl ring on the large redshift of the emission. In other words, the near-UV emission can be altered to a blue emission by simply changing the fused phenyl ring to a naphthyl ring. The PL spectrum of **1** underwent gradual blueshifts as the number of alkyl groups increased, exhibiting blue to sky-blue emissions for **2–5** (λ_{PL} = 472–477 nm). The trend in the blueshifts is reminiscent of those observed in the absorption and electrochemical bandgap of the compounds, thereby exhibiting more blue-shifted emissions for **4** and **5** containing alkyl groups in the azaborine core. All emissions have weak vibronic shoulders due to the ππ* character of their excited singlet states (S_1). Most remarkably, the emission bands are very narrow, with FWHM values of *ca.* 20 nm. Note that the emission profiles of previous dibenzoazaborine systems exhibited FWHM values greater than 28 nm.[25,29] The FWHM being nearly invariant irrespective of alkyl substituents indicates that the rigid benzonaphthoazaborine skeleton is primarily responsible for the narrow emission bandwidths. Moreover, the Stokes shifts of all compounds are small (11 nm), which are comparable to or smaller than those of dibenzoazaborine compounds (>11 nm for **A** in Chart 1),[25,29] although very small values less than 10 nm are known for some azaborine compounds.[30,32] This finding indicates that the effect of photoexcitation on structural relaxation is negligibly small. Benefiting from the rigid and planar structures, all compounds also exhibit near-unity PLQYs. Because the electronic transitions are centered on the azaborine ring core, it is likely that the peripheral alkyl substituents barely affect the PLQY. The transient PL decay profiles of all compounds exhibited a single exponential decay in the nanosecond range (τ = 15.1–17.6 ns), confirming the fluorescence nature of the emission (inset in Fig. 1a and S3†. Furthermore, the highly emissive features of **1–5** were retained in the rigid state (PMMA, 1 wt%), showing the near-unity PLQYs (Fig. S4†). These emission properties, including blue to sky-blue fluorescence, high PLQYs, narrow FWHM values, and small Stokes shifts, could be highly desirable for the use of the planarized *B*,*N*-diarylated benzonaphthoazaborine compounds as potential candidates for blue fluorescent emitters in OLED devices.

Theoretical calculations. To gain a deeper understanding of the photophysical properties of compounds **1–5** in their ground (S_0) and excited (S_1) states, computational studies based on density functional theory (DFT) and time-dependent DFT (TDDFT) were conducted using the PBE0 functional and 6-31+G(d,p) basis set with self-consistent reaction field (SCRF) approximation for taking the influence of solvent medium (toluene) into account. The reference compound **A** was also computationally studied in order to compare its geometric and electronic structures with those of the compounds **1–5**, as shown in Fig. 3. The lowest energy electronic transition can be interpreted to occur between HOMO and LUMO (see Tables S2 and S3†). The HOMO and LUMO for **1–5** exhibit the almost identical spatial distributions; the HOMO has major contributions from the nitrogen atom, phenyl ring, and naphthyl ring, whereas the LUMO is delocalized over the benzonaphthoazaborine and *B*-Ph rings with a significant contribution from the empty p orbital of the boron atom. Thus, the S_1 state formed from the HOMO–LUMO transition can be identified with a ππ* excited state mainly at the benzonaphthoazaborine moiety (Fig. S5†). Although these MO features are similar to those of compound **A**, the extended conjugation through the naphthyl ring in **1–5** elevates the energy levels of HOMOs, whereas it lowers those of LUMOs compared with the corresponding energy levels of **A**. As a result, the bandgaps of **1–5** were significantly reduced by 0.51–0.54 eV compared with that of **A**. Regarding the effects of electronic modifications, the introduction of an electron-donating ^{t}Bu group increases the energy levels of both HOMO and LUMO with different degrees; the influence of ^{t}Bu group attached to the *B*-Ph and *N*-Ph moiety is relatively larger in LUMO and HOMO level, respectively. As a result, the ^{t}Bu group attached to the *B*-Ph (**2**) and further to *N*-Ph moieties (**3**) slightly increases the bandgap by 0.2 and 0.1 eV compared with that of **1**, respectively. The additional attachment of alkyl (Me and ^{t}Bu) groups to the para position of the B-atom in the phenyl ring of benzonaphthoazaborine further destabilizes the LUMO levels (**4** and **5** *vs.* **3**). This result is due to the substantial LUMO participation in the para position of the ring, causing inductive electronic effects of alkyl groups on the LUMO. However, owing to the concurrent elevation of the HOMO levels by the alkyl groups, the increase in the bandgap is marginal. Overall, the computed bandgaps and the absorption and emission wavelengths are qualitatively in accordance with the experimental values. To explain the narrow FWHM values (∼20 nm) of emission spectra measured in the experiment, we examined the structural variations between the S_0 and S_1 states using the optimized geometries of compounds **1–5** and further their reorganization energies.[33–35] All compounds exhibit negligible root-mean-square displacement values of structural deviation (SD_{RMSD}) of 0.022–0.025 Å, which results in insignificant reorganization energies of 0.16–0.17 eV (see Fig. S6†). The SD_{RMSD} and reorganization energies computationally obtained for the compounds **1–5** are comparable to those of narrowband multiple resonance TADF molecules reported in previous literature.[33–35] Therefore, the narrowband emission of compounds **1–5** can be understood with small geometric changes during transition process enough for suppressing non-radiative relaxation.

Finally, we investigated the effect of the naphthyl ring in the azaborine skeleton on aromaticity to confirm the extended π-conjugation effects. To this end, we performed nucleus-independent chemical shift (NICS)[36] calculations for compounds **1** and **A** at the PBE0/6-311++G(d,p) level of theory.[36] The NICS(1) values obtained at 1 Å above the ring centers were used to reduce the local effects of sigma bonds.[37] As shown in Fig. 4, the central BNC4 cores of the two compounds have weak negative values, indicating a weak aromatic character compared with neighboring phenyl rings. The average NICS(1) value for the outer phenyl ring in **1** exhibits a large negative value (−11.3

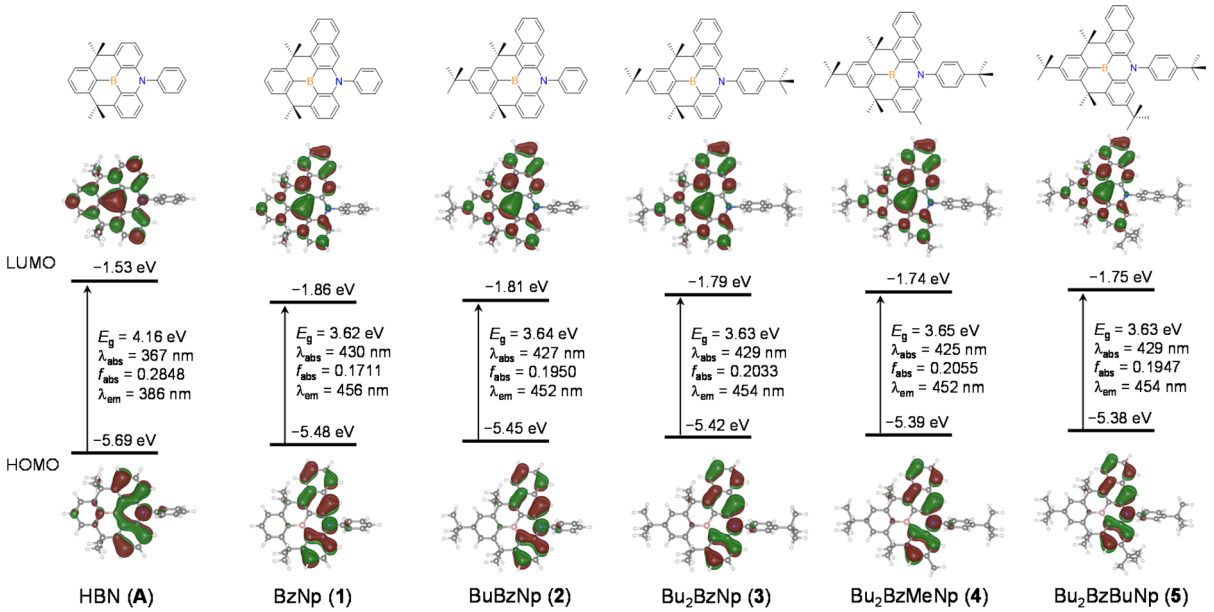

Fig. 3 Frontier molecular orbitals of planarized *B*,*N*-diphenyl dibenzoazaborine (**A**) and *B*,*N*-diarylated benzonaphthoazaborine (**1**–**5**) compounds (isovalue = 0.03) at their ground state (S_0) geometries from PBE0/6-31+G(d,p) calculations. Numerical values of MO energies, HOMO–LUMO bandgaps (E_g), oscillator strengths (f_{abs}), and absorption (λ_{abs}) and emission (λ_{em}) wavelengths are provided.

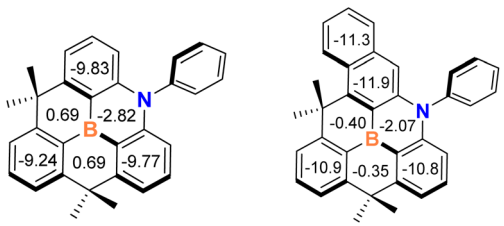

Fig. 4 Calculated nucleus-independent chemical shift [NICS(1)] values of planarized *B*,*N*-diphenyl dibenzoazaborine (**A**, left) and *B*,*N*-diphenyl benzonaphthoazaborine (**1**, right) compounds at the PBE0/6-311++G(d,p)//PBE0/6-31+G(d,p) level of theory.

ppm) which is greater than that of the phenyl ring in **A** (−9.8 ppm). Therefore, this finding indicates that the aromaticity of the azaborine skeleton is enhanced by the incorporation of the naphthyl ring, leading to the reduction of energy gap between HOMO and LUMO.

Conclusions

We demonstrated that the expansion of π-conjugation in the azaborine ring has a significant impact on the photophysical properties of planarized dibenzoazaborine compounds. Replacing one phenyl ring in the dibenzoazaborine core with a naphthyl ring significantly reduced the HOMO–LUMO bandgap, resulting in a shift from near-UV or deep blue to (sky) blue fluorescence. The emission was fine-tuned by attaching electron-donating alkyl groups to the *B*-Ph, *N*-Ph, and/or azaborine rings. It was shown that the electronic effect on the B-centered LUMO level is greater at the azaborine ring than at the *B*-Ph ring. These findings were further explained by electrochemical and theoretical studies. Along with emission tuning, all compounds exhibited high PLQYs, very narrow FWHM values, and small Stokes shifts. The findings of this study will be useful for designing highly fluorescent emitters with high color purity for optical applications.

Conflicts of interest

There are no conflicts of interest to declare.

Acknowledgements

This work was supported by the 2022 Research Fund of University of Ulsan.

Notes and references

1 S. Oda and T. Hatakeyama, *Bull. Chem. Soc. Jpn.*, 2021, **94**, 950–960.
2 S. Madayanad Suresh, D. Hall, D. Beljonne, Y. Olivier and E. Zysman-Colman, *Adv. Funct. Mater.*, 2020, 1908677.
3 J. A. Knöller, G. Meng, X. Wang, D. Hall, A. Pershin, D. Beljonne, Y. Olivier, S. Laschat, E. Zysman-Colman and S. Wang, *Angew. Chem., Int. Ed.*, 2020, **59**, 3156–3160.
4 M. Hirai, N. Tanaka, M. Sakai and S. Yamaguchi, *Chem. Rev.*, 2019, **119**, 8291–8331.
5 X.-Y. Wang, X. Yao, A. Narita and K. Müllen, *Acc. Chem. Res.*, 2019, **52**, 2491–2505.
6 S. K. Mellerup and S. Wang, *Trends Chem.*, 2019, **1**, 77–89.
7 J. Huang and Y. Li, *Front. Chem.*, 2018, **6**, 341.
8 S. M. Parke, M. P. Boone and E. Rivard, *Chem. Commun.*, 2016, **52**, 9485–9505.

9 J. Wagner, P. Zimmermann Crocomo, M. A. Kochman, A. Kubas, P. Data and M. Lindner, *Angew. Chem., Int. Ed.*, 2022, **61**, e202202232.
10 N. Ando, T. Yamada, H. Narita, N. N. Oehlmann, M. Wagner and S. Yamaguchi, *J. Am. Chem. Soc.*, 2021, **143**, 9944–9951.
11 E. von Grotthuss, A. John, T. Kaese and M. Wagner, *Asian J. Org. Chem.*, 2018, **7**, 37–53.
12 A. John, M. Bolte, H.-W. Lerner, G. Meng, S. Wang, T. Peng and M. Wagner, *J. Mater. Chem. C*, 2018, **6**, 10881–10887.
13 D. L. Crossley, R. J. Kahan, S. Endres, A. J. Warner, R. A. Smith, J. Cid, J. J. Dunsford, J. E. Jones, I. Vitorica-Yrezabal and M. J. Ingleson, *Chem. Sci.*, 2017, **8**, 7969–7977.
14 V. M. Hertz, M. Bolte, H.-W. Lerner and M. Wagner, *Angew. Chem., Int. Ed.*, 2015, **54**, 8800–8804.
15 X.-Y. Wang, J.-Y. Wang and J. Pei, *Chem.– Eur. J.*, 2015, **21**, 3528–3539.
16 T. Agou, M. Sekine, J. Kobayashi and T. Kawashima, *Chem. Commun.*, 2009, 1894–1896.
17 T. Agou, T. Kojima, J. Kobayashi and T. Kawashima, *Org. Lett.*, 2009, **11**, 3534–3537.
18 T. Agou, J. Kobayashi and T. Kawashima, *Chem. Commun.*, 2007, 3204–3206.
19 Y. Ishikawa, K. Suzuki, K. Hayashi, S.-y. Nema and M. Yamashita, *Org. Lett.*, 2019, **21**, 1722–1725.
20 P. G. Campbell, A. J. V. Marwitz and S.-Y. Liu, *Angew. Chem., Int. Ed.*, 2012, **51**, 6074–6092.
21 T.-L. Wu, S.-H. Lo, Y.-C. Chang, M.-J. Huang and C.-H. Cheng, *ACS Appl. Mater. Interfaces*, 2019, **11**, 10768–10776.
22 I. S. Park, K. Matsuo, N. Aizawa and T. Yasuda, *Adv. Funct. Mater.*, 2018, **28**, 1802031.
23 Y. Kondo, K. Yoshiura, S. Kitera, H. Nishi, S. Oda, H. Gotoh, Y. Sasada, M. Yanai and T. Hatakeyama, *Nat. Photonics*, 2019, **13**, 678–682.
24 T. Hatakeyama, K. Shiren, K. Nakajima, S. Nomura, S. Nakatsuka, K. Kinoshita, J. Ni, Y. Ono and T. Ikuta, *Adv. Mater.*, 2016, **28**, 2777–2781.
25 M. Ando, M. Sakai, N. Ando, M. Hirai and S. Yamaguchi, *Org. Biomol. Chem.*, 2019, **17**, 5500–5504.
26 V. M. Hertz, N. Ando, M. Hirai, M. Bolte, H.-W. Lerner, S. Yamaguchi and M. Wagner, *Organometallics*, 2017, **36**, 2512–2519.
27 Z. Zhou, A. Wakamiya, T. Kushida and S. Yamaguchi, *J. Am. Chem. Soc.*, 2012, **134**, 4529–4532.
28 S. Saito, K. Matsuo and S. Yamaguchi, *J. Am. Chem. Soc.*, 2012, **134**, 9130–9133.
29 I. N. Istiqomah, H. Mubarok, T. Lee, N. T. N. Nguyen, J. Jung and M. H. Lee, *Bull. Korean Chem. Soc.*, 2022, **43**, 293–298.
30 T. Agou, H. Arai and T. Kawashima, *Chem. Lett.*, 2010, **39**, 612–613.
31 A. Shuto, T. Kushida, T. Fukushima, H. Kaji and S. Yamaguchi, *Org. Lett.*, 2013, **15**, 6234–6237.
32 J.-J. Zhang, L. Yang, F. Liu, Y. Fu, J. Liu, A. A. Popov, J. Ma and X. Feng, *Angew. Chem., Int. Ed.*, 2021, **60**, 25695–25700.
33 X. Cai, J. Xue, C. Li, B. Liang, A. Ying, Y. Tan, S. Gong and Y. Wang, *Angew. Chem., Int. Ed.*, 2022, **61**, e202200337.
34 T. Hua, J. Miao, H. Xia, Z. Huang, X. Cao, N. Li and C. Yang, *Adv. Funct. Mater.*, 2022, **32**, 2201032.
35 G. Meng, H. Dai, T. Huang, J. Wei, J. Zhou, X. Li, X. Wang, X. Hong, C. Yin, X. Zeng, Y. Zhang, D. Yang, D. Ma, G. Li, D. Zhang and L. Duan, *Angew. Chem., Int. Ed.*, 2022, e202207293.
36 Z. Chen, C. S. Wannere, C. Corminboeuf, R. Puchta and P. v. R. Schleyer, *Chem. Rev.*, 2005, **105**, 3842–3888.
37 P. v. R. Schleyer, M. Manoharan, Z.-X. Wang, B. Kiran, H. Jiao, R. Puchta and N. J. R. van Eikema Hommes, *Org. Lett.*, 2001, **3**, 2465–2468.